Energy-drift correction of electron energy-loss spectra from prolonged data accumulation of low SNR signals

Y. Sasano and S. Muto*

Department of Materials, Physics and Energy Engineering, Graduate School of Engineering, Nagoya University, Furo-cho, Chikusa-ku, Nagoya 464-8603, Japan

Abstract

The demand for analysis of trace elements in atomically localized areas by electron energy-loss spectroscopy (EELS) in TEM is increasing. Unfortunately, the prolonged data acquisitions required to achieve acceptable signal-to-noise ratio (SNR) tend to deteriorate the energy resolution because of spectral drifts due to instrumental instability. We developed a macro script for a Gatan Digital Micrograph™ to control an ENFINA 1000 EEL spectrometer that corrects for energy drifts during data accumulation. The script successfully achieved a core-loss spectrum for a sample having ~1 at% elemental concentration, and provided a sufficient SNR for chemical state analysis.

* Corresponding author: TEL:+81 52 789 5200 FAX: +81 52 789 5137 E-mail: s-mutoh@nucl.nagoya-u.ac.jp

Introduction

Electron energy-loss spectroscopy (EELS) is one of the common analytical tools employed in (scanning) transmission electron microscopy ((S)TEM). EELS not only plays a complementary role in elemental analysis to energy-dispersive X-ray analysis (EDXA), but is also capable of chemical state analysis in a highly-localized area because of its high energy resolution. Current key technologies in materials engineering that realize specific properties often rely on segregation of trace elements to atomically localized regions, such as point defects, dislocations, grain boundaries, or surface steps. It is thus crucial to the investigation of functional materials to be able to study exactly where these trace elements occur, and in what quantity. TEM-EELS with associated analytical techniques could be the best and only solution.

Unfortunately, an EELS spectrum is usually accompanied by a high level of background, because there are strong Coulomb interactions between the incoming electron and the atomic charges in the solid, and the cross-sections of core electron excitations are generally small compared to those of the inelastic scattering processes that give rise to the background spectra. The core-loss spectrum from the trace element should hence have an intrinsically low signal-to-background ratio (SBR). On the other hand, in order to obtain spectral data with sufficient signal-to-noise ratio (SNR) from the trace elements, one must either acquire the spectrum with a long exposure time or accumulate a high number of acquisitions, each having a relatively short exposure time. Usually, this prolonged recording results in loss of energy resolution by spectral broadening because each acquisition may exhibit a spectral shift in the energy axis by a few channels, not only due to high voltage instabilities of TEM [1,2] but also due to the environmental effects [3-5]. The latter is extensively discussed in [6] and instrumental

techniques are proposed, which proved to provide dramatic effects on the stability of EELS. On the other hand, a much less expensive alternative to keep the energy resolution intrinsic to the existing spectrometer is to utilize a script program to correct the energy drift and associated peak broadening during the data recording procedure on-line.

There are several control scripts [1,2] available that correct for the energy shift during recording by referring to the energy drift of the elastic peak (zero-loss peak, ZLP) and then displacing the spectrum by the required amount through adjustment of the electrostatic drift tube voltage of the spectrometer. These procedures do not work very well when a core-loss spectrum far from the elastic peak is recorded because the repeated energy shifts required to watch both the elastic peak and the core-loss spectrum of interest cause additional instability of the detector system, as shown in a later section. Moreover when the ELNES of interest from trace elements exhibit very small SNR and SBR, the algorithms are not always effective and the channel-to-channel intensity fluctuation pattern of the detector remains. Precise recognition of the fine spectral structures required for proper chemical state analysis in such cases becomes exceedingly difficult.

In the present article, we present and test scripts on a Digital Micrograph^{TM} (DM) [7], a common instrument control and data processing platform for TEM. The scripts are shown to be effective at accumulating spectral signals with initially low SNR/SBR, and providing output with sufficient SNR for successful chemical state analysis.

Methods

The study is carried out on a JEOL JEM200CX microscope equipped with a Gatan

Enfina1000 spectrometer (CCD size: 1340×100 pixels). The microscope is operated at 200 kV. The energy dispersion of the spectrometer is set at 0.05 eV/channel, the finest energy dispersion available on the ENFINA 1000. The probe size is approximately 300 nm in focused-beam mode and the typical thickness of examined samples is 0.3-0.5 times the respective mean free path for inelastic electron scattering. Spectra are collected in image mode with an energy resolution of 1.2 eV (FWHM of ZLP) using a 3-mm spectrometer entrance aperture. All measurements are conducted following a wait of more than two hours after the TEM and spectrometer startup, to allow for system stabilization. The ZLP position is observed to shift by approximately 60 eV during the warm-up period, after high voltage is applied to the TEM.

The scripts controlling the spectrometer are written in digital micrograph (DM) code, a common environment for Gatan TEM and related spectroscopic instruments [7]. Although data processing in the scripts is applied to the original 2D charge-coupled device (CCD) images of acquired spectra, the output is shown as a 1D projection in the cross-dispersion direction.

Results

Verification of instrumental stability

The position of maximum ZLP is continually monitored after instrument stabilization, as shown in Fig. 1. A single exposure is 1 second. It can be seen that the spectrum can drift by up to approximately ±0.5 eV per minute and ±2 eV per hour. Occasionally, the ZLP exhibits a large change within a single minute of as much as ±3 eV, presumably because of an accidental stray field from an external disturbance or a small electrical discharge within the microscope. This implies that a single spectral

acquisition, taken within a few seconds to tens of seconds exposure time does not significantly deteriorate the spectral resolution, whereas the single acquisition or accumulation of multiple acquisitions, taken with much more total exposure time, in an attempt to increase SNR does adversely lower the energy resolution. This situation is well represented by Fig. 2, in which Mg-K ELNES spectra from $LiNi_{0.8}Co_{0.15}Al_{0.05}O_2$ doped with 1.3 at% Mg (see application section for sample details) are shown, each trial consisting of either a single acquisition of 30 seconds or a successive accumulation of 10 spectra. The single-acquisition spectra are in good agreement with each other within the statistical accuracy of the intensity fluctuations, though their relative positions do shift. On the other hand, the spectral profiles accumulated by 10 acquisitions exhibit significant differences. It is thus clear that corrections for spectral drift during prolonged measurement are necessary to obtain ELNES with sufficient SNR to examine trace elements.

Correction by shifting a reference peak (Script for spectral drift correction, SDC_1)

In order to correct for the effects of energy drift, a DM script is developed to perform several acquisitions followed by internal calibration. First, short-time (typically ~1 second) acquisitions for both a core-loss of interest and a reference peak are performed repeatedly. The energy region is shifted by applying the drift tube to measure the two different spectra. In similar scripts designed to correct for energy drift [1,2] ZLP is used as the reference spectrum because it forms very sharp, recognizable peak in the spectrum and defines the origin of the energy axis, most appropriate for the reference spectrum. When switching from core-loss to low-loss acquisitions, the illumination must be reduced by changing the current in the C2 condenser lens, defocusing the spot

to avoid detector oversaturation. Unfortunately, the lens system of the JEM200CX TEM is not controllable by script. We must therefore use another pre-specified peak, located near the core-loss of interest, as the reference peak when the core-loss is of relatively high energy. A flowchart of the new script is shown in Fig. 3. The process entitled 'collect reference peak' can be repeated any number of times, and the average peak position then used as reference. This script is not intended for measuring the absolute transition energy, but only calibrates the relative energy shift. The procedure for repeated acquisitions of core-loss and reference peak is very similar to that used in the previously reported scripts [1,2], except for the use of an arbitrary reference peak instead of the ZLP.

In an ENFINA 1000 spectrometer, the energy region can be shifted by applying either the electrostatic drift tube or a magnetic field (by checking the 'magnetic' box on the floating window of 'FilterControl'). The energy shift caused by the drift tube is limited to less than 1000 eV. If the required energy shift exceeds 1000 eV, the spectrometer automatically assigns the appropriate energy shift values to both the drift tube and the sector magnet. It is then necessary to examine whether the spectral peak returns to its initial position after switching from core-loss to reference peak acquisition, and applying the drift tube or magnetic field. The results are shown in Figs. 4(a) and (b), where the peak location of the ZLP is monitored by first setting it at the channel of 100 for 1 minute, and then applying a magnetic or drift tube value of 1000 eV for 10 s, and finally reducing the applied energy shift back to 0 eV. As expected, the magnetic shift exhibits an energy gap of 1-2 eV between the initial and final ZLP position just after shifting ZLP forth and back by 1000 eV. It takes more than ten minutes for the ZLP to return to its initial position, probably due to the large hysteresis of the spectrometer's

sector magnet. In the results presented, the script always changed the drift tube voltage to shift the energy between the reference peak and core-loss acquisitions, which limited the energy difference between the two spectra to 1000 eV. Since a small, discontinuous ZLP shift is observed when switching the drift tube on, the script sets a delay of ten seconds after shifting the energy region from the reference peak to the core-loss of interest.

The experimental spectra from the same sample shown in Fig. 2 are shown in Fig. 5, where a single acquisition with an exposure of 30 seconds and a set of 10 acquisitions accumulated using the developed script are overlaid. The input parameters are listed in Table 1. The spectral position and profile show no significant shift and the energy shift correction is performed successfully. However, this script has several problems:

(i) The energy shift due to instrumental instabilities is found by measuring the shift of a reference peak located within 1000 eV of the core-loss of interest. The accuracy of this shift is highly dependent on both the sharpness and SNR of the reference peak. It can be difficult to identify an appropriate reference peak, as it must be sufficiently sharp, have acceptable SNR, and be located within 1000 eV of the objective core-loss.

(ii) There is no guarantee that the energy shift observed for the reference peak is equal to that of the objective core-loss spectrum because there can be accidental energy instabilities during the energy shift from the reference to the objective spectrum by applying the drift tube voltage.

(iii) The script performs acquisition of the reference peak, a timed delay, and finally the acquisition of the objective spectrum. This usually takes about three times longer than the acquisition of the objective spectrum using simple data accumulation, and may result in increased irradiation damage to the sample.

Another algorithm is devised to correct for energy drift, while avoiding the above difficulties.

Drift correction by cross-correlation between consecutive acquisitions (SDC_2)

In the previous section, energy drift was corrected by referring to the shift of a reference peak, though it is desirable to avoid changing the drift tube voltage because of the resulting temporal instabilities of the detector. It is thus preferable to measure the energy drift directly from the core-loss spectrum. Cross correlation is a standard method of calculating the degree to which two series of datasets are correlated. The cross correlation function CCF, usually used to compare two images, $f(x, y)$ and $g(x, y)$, is defined as [8]:

$$\mathrm{CCF} = \sum_{x,y} \frac{\left[f(x,y) - \bar{f}\right]\left[g(x,y) - \bar{g}\right]}{\sigma_f \sigma_g}, \qquad (1)$$

where $\bar{f}$ and $\bar{g}$ are the means of $f(x, y)$ and $g(x, y)$, and σ_x and σ_y are the standard deviations of all the pixel values in $f(x, y)$ and $g(x, y)$. This function is sometimes described as 'normalized cross correlation', where $-1 \le \mathrm{CCF} \le 1$, the bounds indicating maximum correlation and 0 indicating no correlation. A high negative correlation indicates a high correlation but of the inverse of one of the series. In the present case, the images correspond to the CCD images of acquired spectra and the summation is conducted only about the dispersion direction (x direction). Terada *et al* [9] applied a similar CCF technique to spatially-resolved EELS *after* recording a number of time-resolved data not only to improve the data SNR but also correct the spatial drift.

For this technique to apply to the measurement of low SNR/SBR spectra, the signal level of the objective core-loss edge of interest should be well above the noise level, and

thus the noise distribution in the detector should be examined. The cross correlation between two series of data, each acquired for 10 seconds, under uniform illumination (dispersion = 0 eV/channel mode), and after dark current correction and gain normalization is shown in Fig. 6(a). Although no core-loss spectrum is included, and thus no significant correlation is expected, a sharp peak at the origin is observed, indicating that the intensity fluctuation patterns in the first and second acquisitions show a strong correlation. The recorded intensity fluctuation patterns of the first and second acquisitions are shown in Fig. 6(b). The intensity fluctuations at the wavelength of ~10 channels show a strong correlation through the entire series of data acquisitions. The standard deviation of intensity fluctuations can be reduced by increasing the number of acquisitions by conducting the routine 'PREPEARE GAIN REFERENCE' on the DM menu, though the standard deviation still amounts to 0.6-0.9% of the average count. This is a significant amount of noise because the signal level of trace elements is often 1% or less of the average count level. To illustrate the problem more clearly, CCF is calculated for actual spectral data: two Ni $L_{2,3}$ ELNES spectra from a NiO thin film recorded consecutively by deliberately reducing the beam current and deteriorating the SNR are shown in Fig. 7(a), and the CCF of the two spectra is shown in Fig. 7(b). A small but cusped maximum always occurs at the origin, originating from the high correlation of the intrinsic intensity fluctuation. This makes the location of the exact maximum correlation position (the maximum of the broad peak) problematic. This problem is easily solved by applying Fourier filtering to the CCF, cutting the high-frequency components. The width of the low-pass filter in Fourier space can be specified in a pop-up window, with the typical value being ~10 channels. A resulting smoothed CCF is shown in Fig. 7(c), where the energy drift of the spectrum can be

more easily specified at the location of maximum CCF. Recently Bosman and Keast [10] intensively discussed the source of such systematic noise derived from the gain reference image of an EELS system. They developed a sophisticated method, 'binned gain averaging,' which increases spectrum acquisition speed and spectral sensitivity. This method can be used in advance before applying the present script in data acquisition, which will improve SNR even better and/or it might allows us to skip the smoothing CCF procesure.

To accelerate the calculation of CCF for each spectral acquisition, we take advantage of a pre-existing command in the DM scripting language: equation (1) can be rewritten as [8]:

$$CCF = \left\langle \frac{F}{\|F\|}, \frac{G}{\|G\|} \right\rangle, \qquad (2)$$

where

$$F(x, y) = f(x, y) - \bar{f},$$

$$G(x, y) = g(x, y) - \bar{g},$$

< , > is the inner product (dot product) and || || is the Euclidian norm. The mathematical operations of mean, standard deviation, and inner product of arrays can be readily conducted by the script commands 'Mean', 'RMS' and 'Dotproduct' of the specified 1D or 2D arrays [7], accelerating the CCF calculation by two orders of magnitude compared to the same calculation using 'for' loops.

A flowchart of the script is shown in Fig. 8, and a list of input parameters is tabulated in Table 2. One can first select whether ZLP position calibration is conducted to correctly locate the origin of the energy loss axis before core-loss measurements begin. However, this calibration does not necessarily guarantee that the measured

core-loss energy loss is correct because of reason (ii) in the previous section. The second option given is whether to use a reference peak to monitor the energy drifts. This option can be useful if the SNR of the spectrum is nearly unity at a single acquisition and a sharp peak of another constituent element is located nearby.

Once the parameters are set, the CCF of the second acquisition with the first acquisition is calculated, and the two spectra are summed with the second spectrum numerically displaced by the energy shift in the dispersion direction, rather than physically shifted by the application of a drift tube voltage. For the third acquisition, the CCF of the newly acquired spectrum with the previously summed spectra is calculated and the new acquisition is then shifted and summed with the previously accumulated spectra unless the energy shift between the two most recent acquisitions is larger than a preset limit (*Energy shift limit*). The procedure is repeated until a specified number of iterations is reached. Each newly acquired core-loss spectra is abandoned without inclusion in the spectral summation if it is shifted by more than the specified *Energy shift limit*, because such an unusually large energy drift would likely be caused by accidental irregularities in the measurement, and the inclusion of such an acquisition would distort the spectral profile.

As a test of the script, the Ni $L_{2,3}$ ELNES shown in Fig. 6(a) is accumulated 100 times. The input values for the preset parameters and instrumental conditions are listed in Table 2, and the accumulated spectrum together with a single acquisition is shown in Fig. 9(a). A single acquisition under a focused beam condition is also shown in the figure. The monitored energy drift value and the maximum value of CCF for every acquisition are respectively shown in Fig. 9(b) and (c). The spectral position on the CCD can shift by as much as ~4 eV (80 channels) during 100 acquisitions, though the

resultant shifted spectrum exhibits no significant loss of energy resolution. The CCF maximum exhibits relatively small values for the first cumulative acquisition because the first two consecutive acquisitions have low SNR. The CCF maximum values stabilize after 10 to 20 acquisitions at more than 0.9 because the CCF of each new acquisition is calculated with the previously accumulated spectrum. Note that, compared to the previous results shown in Fig. 5, the SNR is significantly improved in the accumulated spectrum because of the averaging out of pixel-to-pixel gain variation by the summation of many spectra displaced by the number of shifted channels, the effect of which is already demonstrated in [11,12].

The present developed script only monitors the spectral shift occurring between consecutive acquisitions, though spectral broadening may also occur during a single acquisition due to the energy drift for a long exposure time. This can be, in principle, also monitored by watching out every calculated cross-correlation value and any single acquisition should be discarded when the calculated cross-correlation value is less than a specified value. The same effect can be obtained just by decreasing the value of the pre-specified parameter '*Energy shift limit*,' because the broadened spectrum will provide a larger energy shift value. We usually set the single exposure time less than 30 seconds and this setting reveals the spectral broadening no larger than 0.2 eV after the whole system is well stabilized, according to the data in Fig. 1, which practically does little harm to the required chemical analysis.

Application of EDC_2 to trace element analysis

ELNES of doped Mg in a positive electrode active material for use in a lithium ion secondary battery

The developed script was applied to an actual problem: ELNES analysis of a trace

element. The sample is $LiNi_{0.8}Co_{0.15}Al_{0.05}O_2$ doped with 1.3 at% Mg [13], and Mg K ELNES is measured. The raw spectrum of a single acquisition with an exposure of 30 seconds and the Mg K signal, extracted by subtracting the pre-edge background, are shown in Fig. 10. The signal-to-background ratio is ~1%. The resultant spectra accumulated by 10 and 200 acquisitions are shown in Figs. 11(a) and (b), respectively, and the input parameters are listed in Table 2. The total acquisition times were approximately 310 and 6050 seconds, respectively, indicating that the CCF computation time is almost negligible.

The spectra of Fig. 11 were PIXON-deconvolved with the low-loss spectra to improve the energy resolution [14,15], the results of which are shown in Fig. 12 together with XANES from the same sample, in which the energy resolution is estimated to be 0.2 eV. The fine structures are in good agreement with XANES and the spectral quality is good enough to be compared with theoretical predictions of the spectral profile [13,15]. The detailed analysis is reported elsewhere [13], where ELNES were successfully obtained from samples with trace element composition as low as ~0.6 at% with sufficient SNR to allow comparison with theoretical predictions [13].

Notes for GIF TRIDIUM users

The present scripts also work in a Gatan Image Filter TRIDIUM with the following caveats. Be sure to specify the effective CCD area according to the respective spectrometer setting. Also ensure that the drift tube check box is always checked when using the scripts, because the check may be automatically cancelled when switching the spectrometer from the TEM mode to the spectroscopy mode.

Concluding remarks

Methods to correct for spectral drift during prolonged acquisition of EELS ionization edges and to accumulate a series of acquisitions to achieve acceptable SNR have been developed for implementation in a standard post-column TEM-EELS system using DigitalMicrograph^{TM} scripts. The scripts successfully correct for spectral drifts even in spectra of trace elements at ~1 at% or less, and provide sufficient SNR for comparison with theoretical predictions. The scripts are available upon request from the corresponding author by e-mail.

Acknowledgments

This study was supported in part by Grants-in-Aid for Scientific Research (KAKENHI) on Priority Areas, "Nano Materials Science for Atomic Scale Modification 474", "Kibankenkyu A" and "Houga-kenkyu" from Ministry of Education, Culture, Sports, Science and Technology (MEXT) of Japan. The LiNiCoAl(Mg)O_2 sample is supplied by Dr. T. Sasaki of Toyota Central R & D Laboratories Inc. and the XANES in Fig. 12 was measured by Dr. T. Yoshida at the BL1A station at UVSOR in the Institute for Molecular Science, Okazaki, Japan, to whom many thanks are due.

Appendix Spike noise removal

Since the scripts developed in the present study are intended to measure a spectrum with low SNR, noise sources for the CCD detector should be examined. After the detector is sufficiently cooled and dark count and gain corrections are conducted, the only significant noise sources are the signal readout noise and the inevitable photon shot noise. Since the readout noise is independent of the duration of exposure, longer exposure in principle provides a better signal-to-noise (S/N) ratio. However, exposure time is practically limited by spike noise, which is generated by cosmic rays or possibly γ- and/or α-rays emitted from materials around the detector chip [16]. Such high-energy rays striking the CCD chip usually generate thousands of electrons per quantum in a pixel, while a single photon absorbed by the detector produces less than one electron on average. Thus the spike noise can easily obscure a spectrum with low SNR.

An example of an accumulated spectrum using the EDC_2 script is shown in Fig. A-1. Dark dots are seen in a row (indicated by an arrow) in the CCD image (a) and (b). Currently, the spike noise is included in the gain reference image. The projected 1D spectrum of (a) is shown as a black solid line in (c), and the spike noise is overlaid at the core-loss edge. Spike noise should therefore be distinguished from true photon signals, and a reliable method to eliminate spikes is required. A simple and efficient 'median filter' method is applied to eliminate spike noise from CCD data without losing the original spectral information collected by the EDC_2 script.

The median filter is a non-linear digital filtering technique, often used to remove noise from images or other signals. The method is performed using a window consisting of an odd number of samples. The values in the window are sorted into numerical order; the median value, i.e., the sample in the center of the window, is selected as the output.

The oldest sample is discarded, a new sample acquired, and the calculation repeats for all the image pixels. We apply a 3 pixel × 3 pixel window, and the following procedure:

(i) Apply the median filter to the 2D spectral image.

(ii) Calculate the difference image between the original and median-filtered images.

(iii) If any pixel's absolute value in the difference image is larger than three times the mean square root of the difference image intensities, those pixel values in the original image are replaced by those from the median-filtered image at the same location. This effectively removes only pixels with anomalous intensities, beyond expected statistical error.

The resultant projected 1D spectrum is shown as a red line and the removed spike noise is shown as a blue line in Fig. A-1(b). The procedure above is also coded as a DM script, which was applied to all spectral results in the present paper.

References

1 Kimoto K, and Matsui Y (2002) Software techniques for EELS to realize about 0.3 eV energy resolution using 300 kV FEG-TEM. *J. Microsc*. **208**, 224-228.

2 Potapov P L and Schryvers D (2004) Measuring the absolute position of EELS ionisation edges in a TEM. *Ultramicrosc*. **99**, 73-85.

3 Hetherington C J, Cullis A G, Walker S, Turner J, Nelson E C and O'Keefe M A (1998) Installing and operating FEGTEMs. *Mater. Res. Soc*. Boston **523**, 171-176.

4 Muller D A and Grazul J (2001) Optimizing the environment for sub-0.2 nm scanning transmission electron microscopy. *Jpn. Soc. Electron Microsc*. **50**, 219-226.

5. O'Keefe M A, Turner J H, Musante J A, Hetherington C J D, Cullis A G, Carragher B, Jenkins R, Milgrim J, Milligan R A, Potter C S, Allard L F, Blom D A, Degenhardt L, Sides W H (2004) Laboratory design for high-performance electron microscopy. *Microscopy Today* May, 8.

6 Yuan J, Wang Z, Fu X, Xie L, Sun Y, Gao S, Jiang J, Hu X and Xu C (2008) Development of electron energy-loss spectroscopy for nanoscience. *Micron* in press, and references therein.

7 Useful information on Gatan DM and scripting is found in :
http://www.felmi-zfe.tugraz.at/dm_scripts/welcome.html

8 Ballad D H (1982) *Computer vision*. pp. 65-70, (Prentice Hall, Inc., Englewood Cliffs)

9 Terada S, Aoyama T, Yano F and Mitsui Y (2002) Time-resolved acquisition technique for spatially-resolved electron energy-loss spectroscopy by energy-resolved TEM. *J. Electron Microsc*. **51**, 291-26.

10 Bosman M and Keast V J (2008) Optimizing EELS acquisition. *Ultramicrosc*. in

press.

11 Hicks P J, Daviel S, Wallbank B and Comer J (1980) An electron spectrometer using a new multidetector system based on a charge-coupled imaging device. *J. Phys*. E **13**, 713-715.

12 Shuman H and Kruit P (1985) Quantitative data processing of parallel recorded electron energy - loss spectra with low signal to background. Rev. Sci. Instrum. 56, 231-239.

13 Tatsumi K, Sasano Y, Muto S, Yoshida T, Sasaki T, Horibuchi K, Takeuchi Y and Ukyo Y (2008) Local atomic and electronic structures around Mg and Al dopants in lithium-nickel oxide electrodes studied by XANES/ELNES and first-principles calculations. *Phys. Rev. B*, accepted.

14 Muto S, Puetter R C and Tatsumi K (2006) Spectral restoration and energy resolution improvement of electron energy-loss spectra by Pixon reconstruction: I. Principle and test examples. *J. Electron Microsc*. **55**, 215-223

15 Muto S, Tatsumi K, Puetter R C, Yoshida T, Yamamoto Y and Sasano Y (2006) Spectral restoration and energy resolution improvement of electron energy-loss spectra by Pixon reconstruction: II. Application to practical ELNES analysis of low SNR. *J. Electron Microsc*. **55**, 225-230.

16 Bilhorn R B, Sweedler J V, Epperson P M and Denton M B (1987) Charge Transfer Device Detectors for Analytical Optical Spectroscopy — Operation and Characteristics. *Appl. Spectrosc*. **41**, 1114-1125.

.

Figure captions

Fig. 1 ZLP position versus time, measured at a rate of 12 times per minute with an exposure time of 0.1 s.

Fig. 2 Comparison between a single acquisition of 30 seconds (grey lines) and a successive accumulated spectrum of 10 spectra (red lines) for two separate measurements of Mg K edge, with the pre-edge background subtracted. The vertical scale for the accumulated spectra is reduced by 1/10. The energy-loss axis is not calibrated.

Fig. 3 Flow chart for spectral drift compensation by the reference peak method.

Fig. 4 Monitored ZLP position after shifting the ZLP by 1000 eV, holding the voltage for 10 seconds, and then canceling the applied voltage, using magnetic (a) and electrostatic drift tube (b).

Fig. 5 Comparison between a single acquisition (gray line) of 30 seconds and a successive accumulation of 10 spectra (red line) with a single exposure of 30 s for the Mg K edge, using a script to apply the reference peak method. The pre-edge background is subtracted. The Ni L_3 peak is used as the reference. The vertical scale for the accumulated spectra is reduced by 1/10.

Fig. 6 (a) Cross correlation function (CCF) between two consecutive acquisitions of

gain reference patterns with uniform illumination of the detector. (b) Central 100 pixels extracted from the gain reference patterns.

Fig. 7 (a) Ni $L_{2,3}$ spectra collected under reduced electron beam, vertically shifted to align to each other. (b) CCF between the two spectra in (a). Note the sharp peak at the origin indicated by an arrow. (c) Smoothed CCF by applying Fourier low-pass filter (red line) overlaid on the original non-filtered CCF (black line). Note that the true correlation's maximum position can be easily specified as indicated by an arrow.

Fig. 8 Flow chart for EDC_2 script obtained by the CCF method.

Fig. 9 (a) Single acquisition with reduced intensity at an exposure time of 10 s (grey line, scaled by 10 times), final spectrum accumulated 100 times using the EDC_2 script (CCF method) (red line) and single acquisition with the focused beam at an exposure time of 10 s (black line, shifted upwards for visibility). The pre-edge background is subtracted for each spectrum. (b) Spectral shift at each cumulative acquisition measured by the CCF maximum position relative to the first acquisition. (c) CCF maximum values at each cumulative acquisition.

Fig. 10 Raw data (red line) of Mg K edge from a $LiNi_{0.8}Co_{0.15}Al_{0.05}(Mg_{0.05})lO_2$ thin foil sample, acquired with an exposure time of 30 s. The power law background is drawn to better observe the signal-to-background ratio.

Fig. 11 Single acquisition with reduced intensity and an exposure time of 30 s (grey line,

scaled by 10 times (a) and by 200 times (b)), final spectrum accumulated 10 (a) and 200 times (b), using the EDC_2 script (red line).

Fig. 12 Comparison between XANES spectrum taken from the $LiNi_{0.8}Co_{0.15}Al_{0.05}(Mg_{0.05})O_2$ powder [7] and ELNES of Fig. 11(b), deconvolved by the Pixon method to improve energy resolution.

Fig. A-1(a) CCD image of EEL spectrum, accumulated using EDC_2 script. The arrow indicates the position of dark dots caused by spike noise while recording the gain reference image. (b) 1D projection of (a) in the cross dispersion direction (black line) and after spike removal (red line). The removed noise is also shown (blue line).

Table 1 List of input parameters to EDC_1 for acquiring the data shown in Fig. 5. Users can input these parameters to pop-up windows that appear after starting the script.

Parameter name	Description	Input values
Data title	Title appearing on the data window tab	Test for Mg
Element name	Name of objective element	Mg
Start energy	Energy loss value at the left bound of CCD in eV.	1250
Exposure time	Exposure time for each single acquisition in seconds	30
# of acquisitions	Number of data acquisitions for accumulation	10
Ref. element name	Name of element for reference peak	Ni
Ref. start energy	Energy loss value at the left bound of CCD in eV for recording the ref. peak	840
Ref. peak energy	Peak position of the ref. peak to be located in eV	858
Ref. exposure time	Exposure time for each single acquisition of ref. peak in seconds	5
# of Ref. acquisitions	Number of ref. peak acquisitions for averaging	1
Energy shift limit	The newly acquired data is abandoned if the ref. peak is shifted by larger than this value in eV	0.2

Table 2 List of input parameters for acquiring the data in Fig. 9(a) (3rd column) and Fig. 11 (4th column).

Parameter name	Description	Input values	
Data title	Title appearing on the data window tab	Test for Ni	Mg-K
Element name	Name of objective element	Ni	Mg
Start energy	Energy loss value at the left bound of CCD in eV.	830	1325
Exposure time	Exposure time for each single acquisition in seconds	10	30
Energy shift limit	The newly acquired data is abandoned if the ref. peak is shifted by larger than this value in eV	0.2	0.2
# of acquisitions	Number of data acquisitions for accumulation	100	10(200)
CCF start energy	Specify in eV the energy region for which CCF is calculated	850	1330
CCF end energy		885	1365
Low pass filter width	Low pass filter width in # of channels	10	10

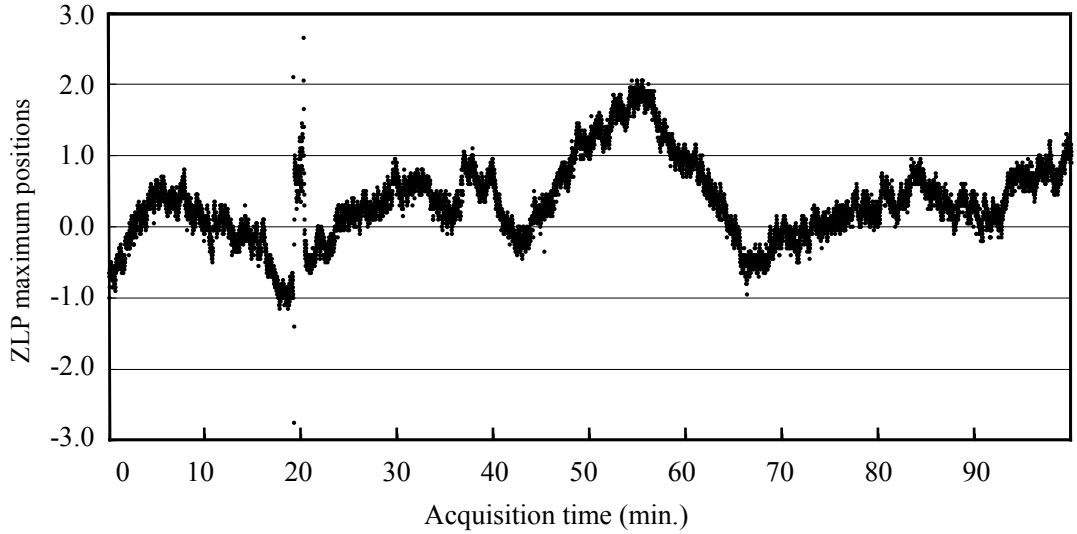

Fig. 1 ZLP position versus time, measured at a rate of 12 times per minute with an exposure time of 0.1 s.

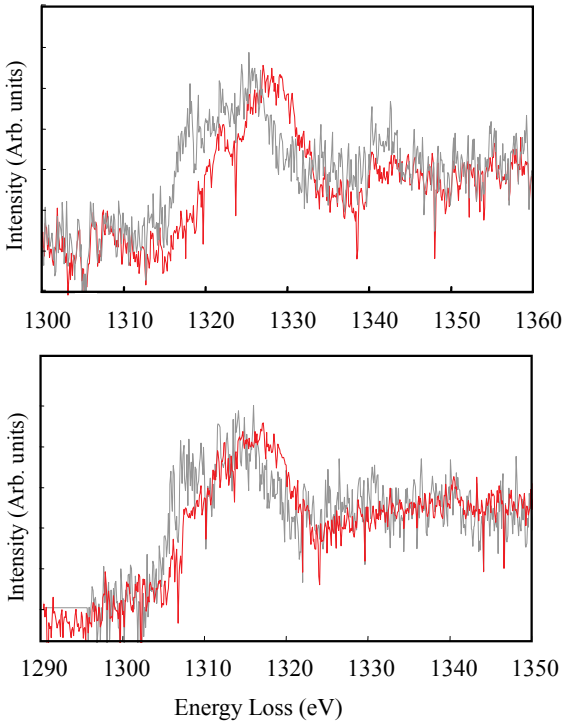

Fig. 2 Comparison between a single acquisition of 30 seconds (grey lines) and a successive accumulated spectrum of 10 spectra (red lines) for two separate measurements of Mg K edge, with the pre-edge background subtracted. The vertical scale for the accumulated spectra is reduced by 1/10. The energy-loss axis is not calibrated.

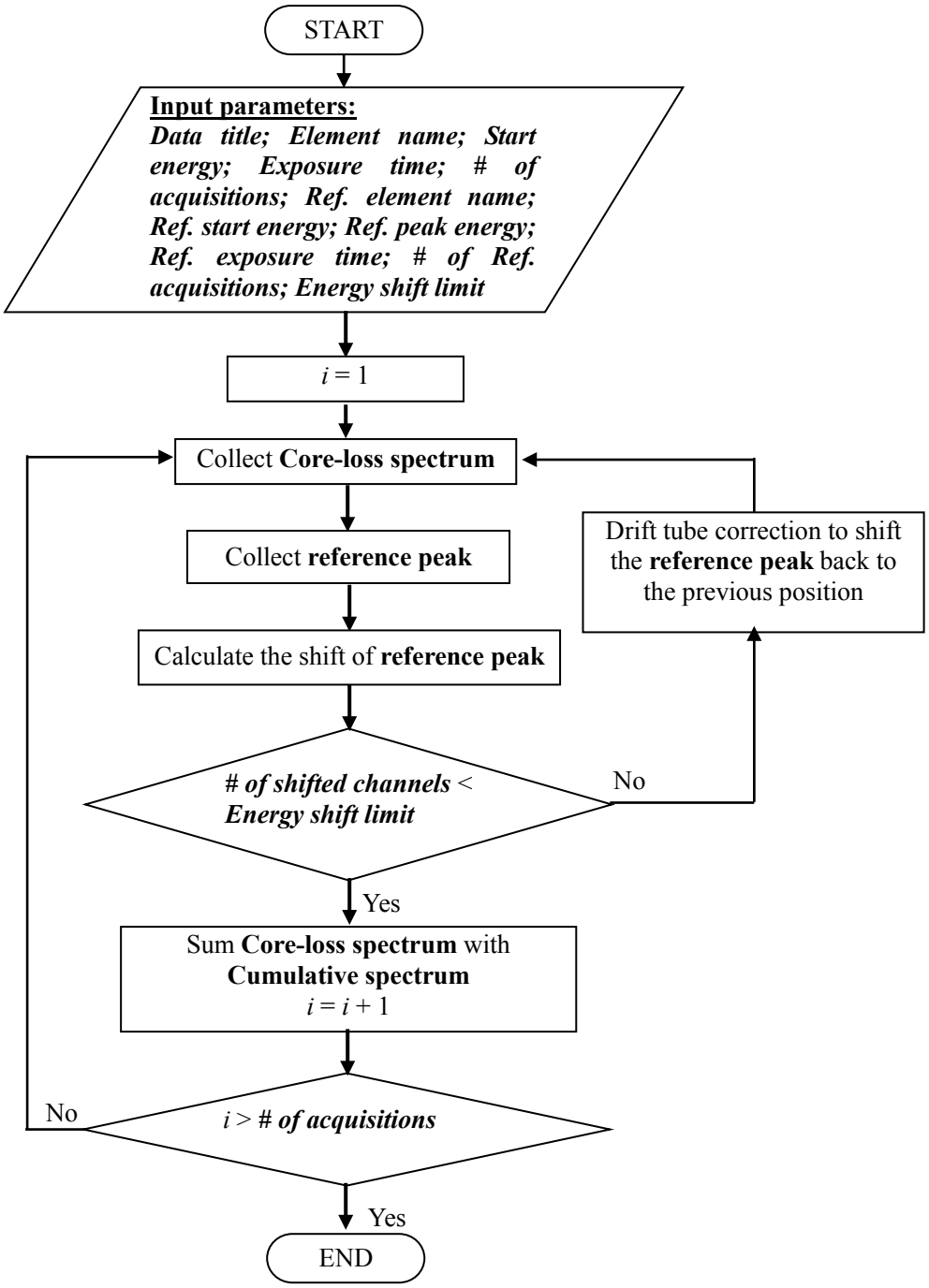

Fig. 3 Flow chart for spectral drift compensation by the reference peak method.

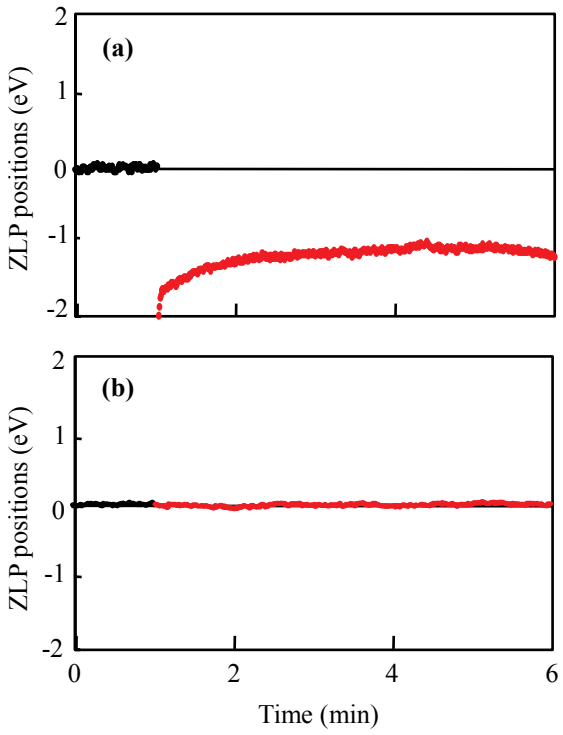

Fig. 4 Monitored ZLP position after shifting the ZLP by 1000 eV, holding the voltage for 10 seconds, and then canceling the applied voltage, using magnetic (a) and electrostatic drift tube (b).

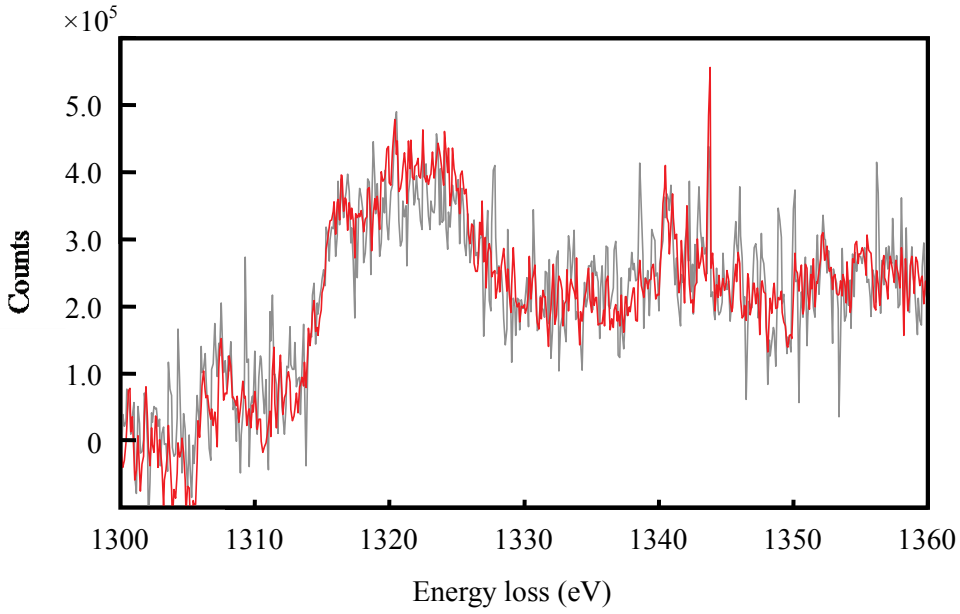

Fig. 5 Comparison between a single acquisition (gray line) of 30 seconds and a successive accumulation of 10 spectra (red line) with a single exposure of 30 s for the Mg K edge, using a script to apply the reference peak method. The pre-edge background is subtracted. The Ni L_3 peak is used as the reference. The vertical scale for the accumulated spectra is reduced by 1/10.

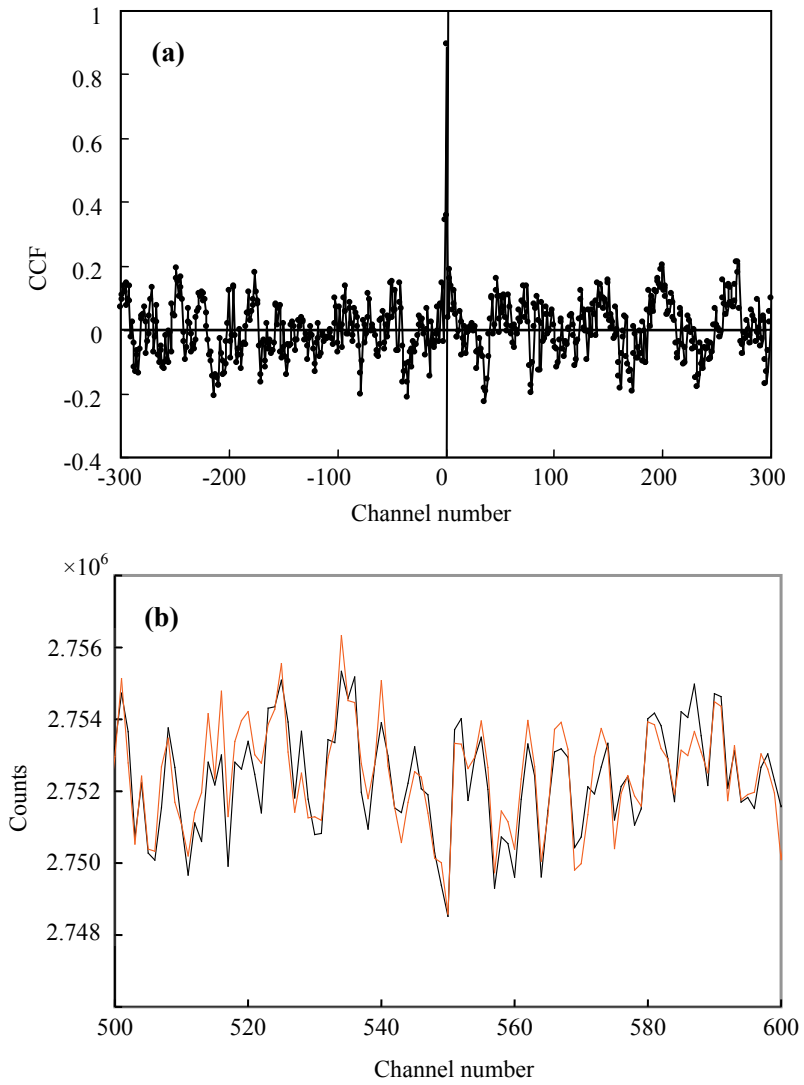

Fig. 6 (a) Cross correlation function (CCF) between two consecutive acquisitions of gain reference patterns with uniform illumination of the detector. (b) Central 100 pixels extracted from the gain reference patterns.

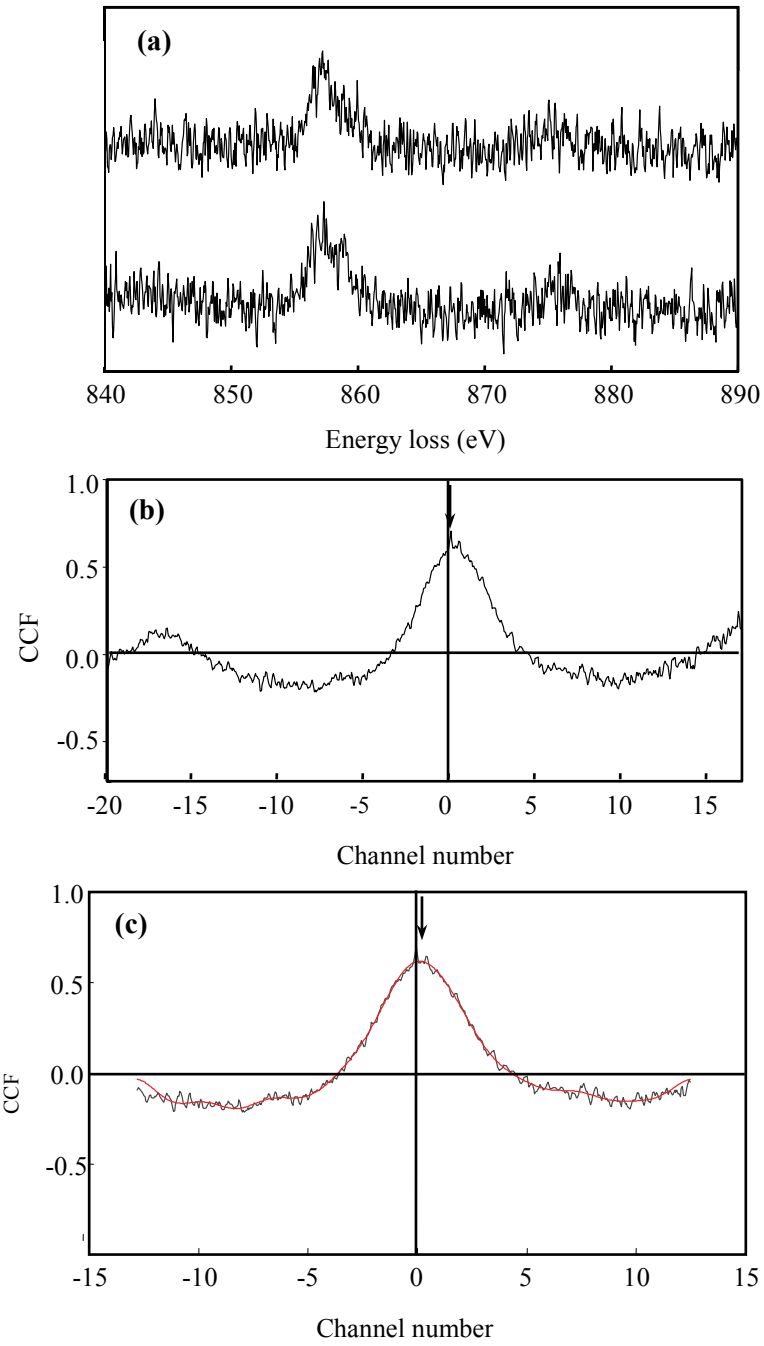

Fig. 7 (a) Ni $L_{2,3}$ spectra collected under reduced electron beam, vertically shifted to align to each other. (b) CCF between the two spectra in (a). Note the sharp peak at the origin indicated by an arrow. (c) Smoothed CCF by applying Fourier low-pass filter (red line) overlaid on the original non-filtered CCF (black line). Note that the true correlation's maximum position can be easily specified as indicated by an arrow.

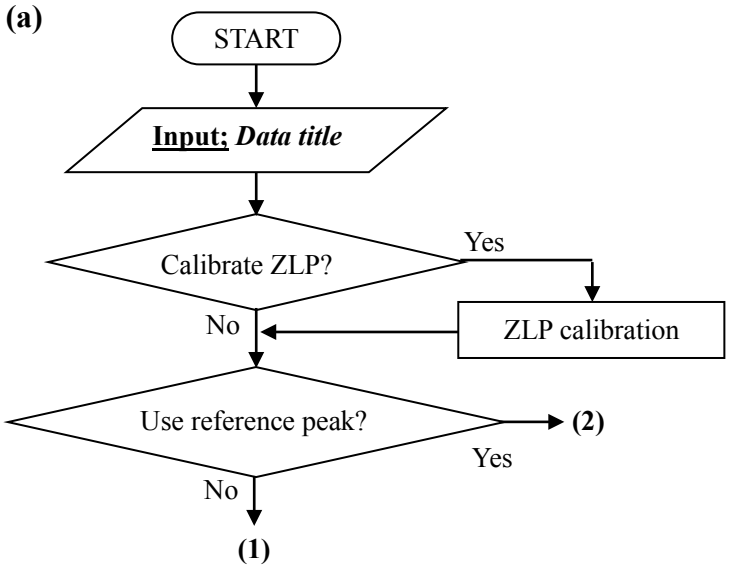

Fig. 8 Flow chart for EDC_2 script obtained by the CCF method.

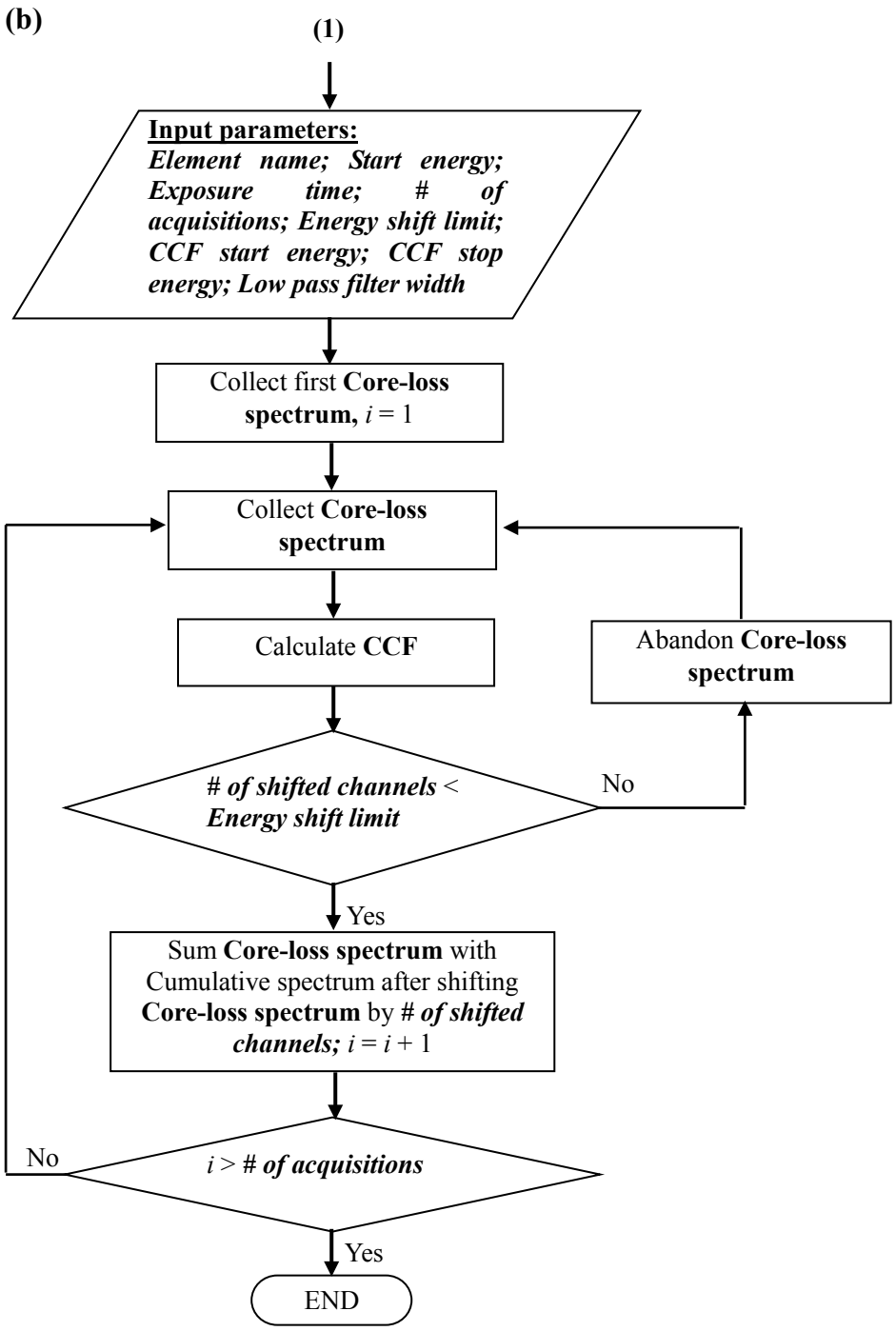

Fig. 8 (continued)

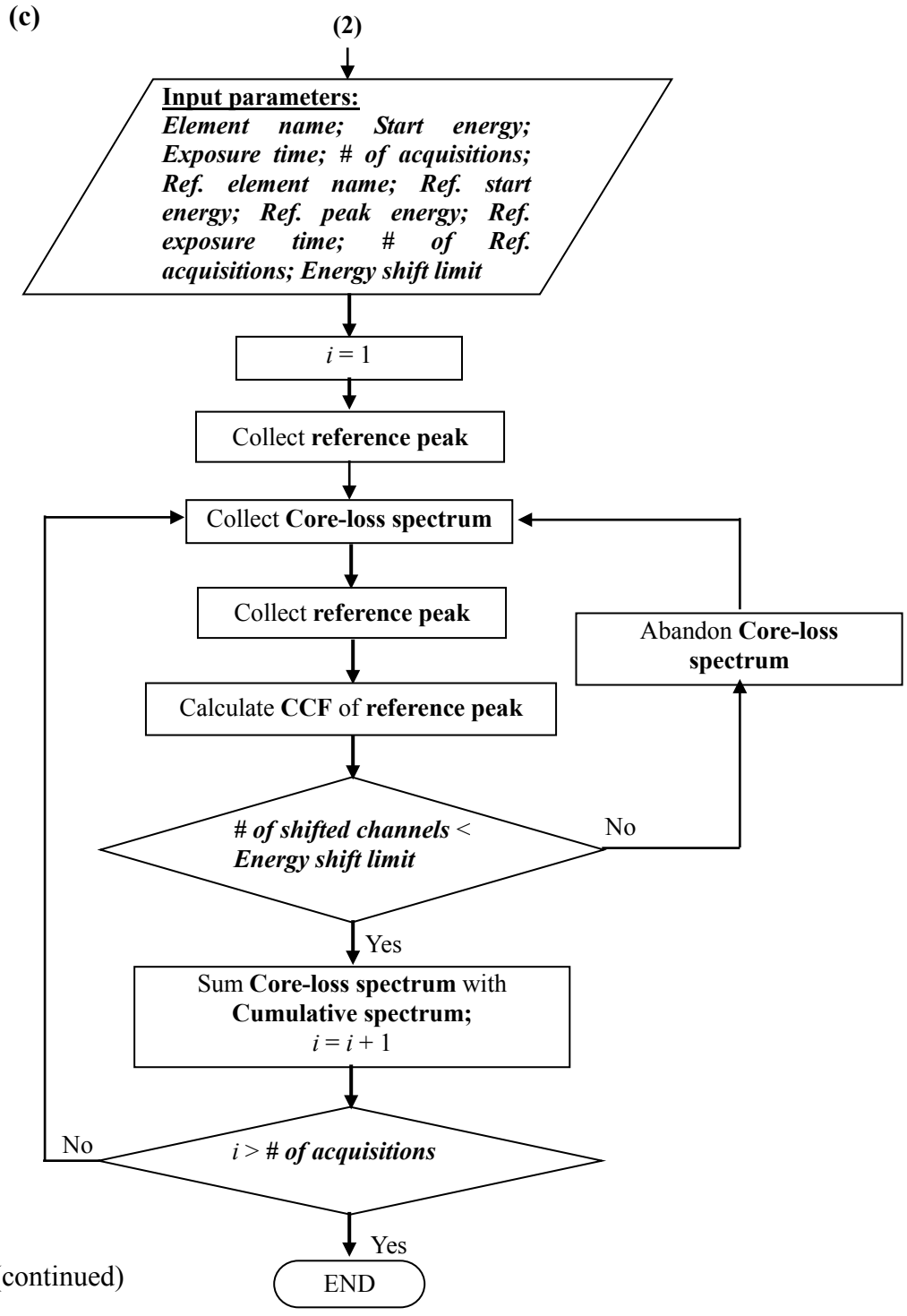

Fig. 8 (continued)

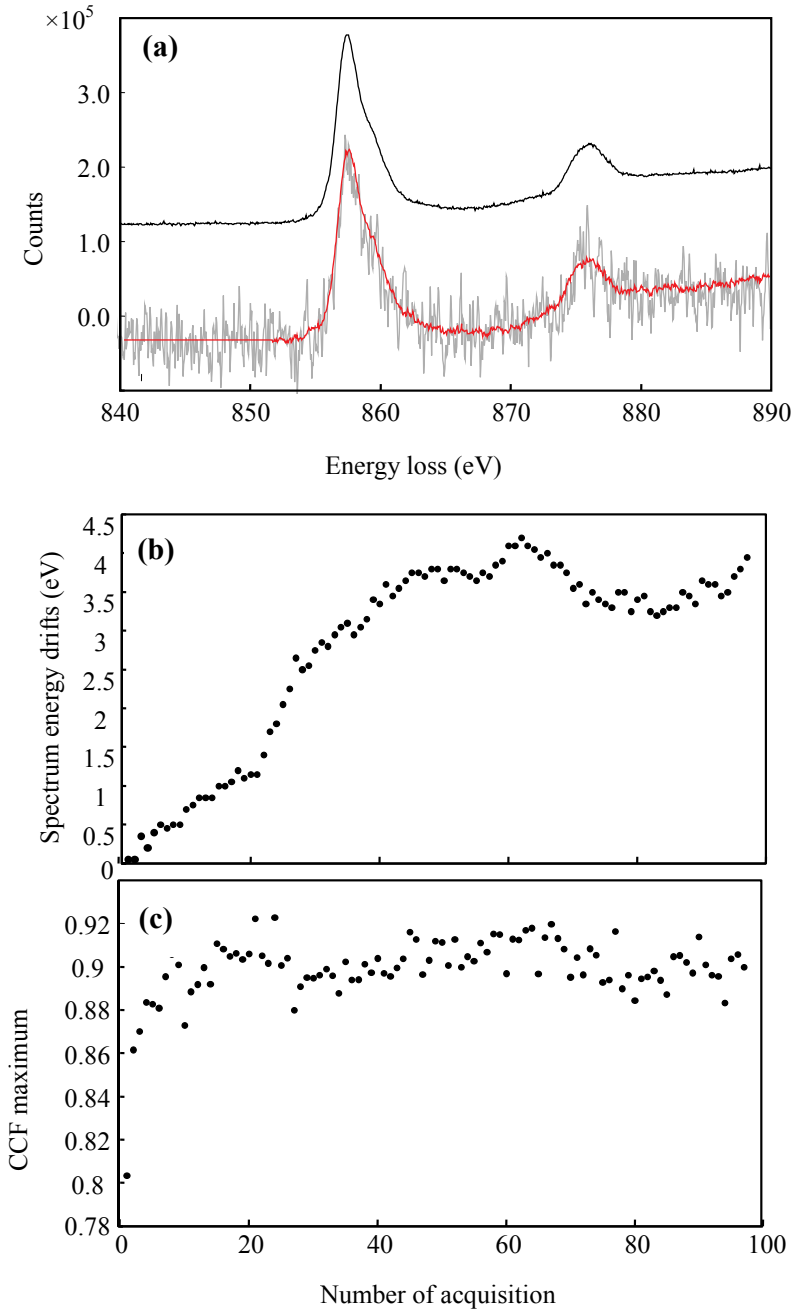

Fig. 9 (a) Single acquisition with reduced intensity at an exposure time of 10 s (grey line, scaled by 10 times), final spectrum accumulated 100 times using the EDC_2 script (CCF method) (red line) and single acquisition with the focused beam at an exposure time of 10 s (black line, shifted upwards for visibility). The pre-edge background is subtracted for each spectrum. (b) Spectral shift at each cumulative acquisition measured by the CCF maximum position relative to the first acquisition. (c) CCF maximum values at each cumulative acquisition.

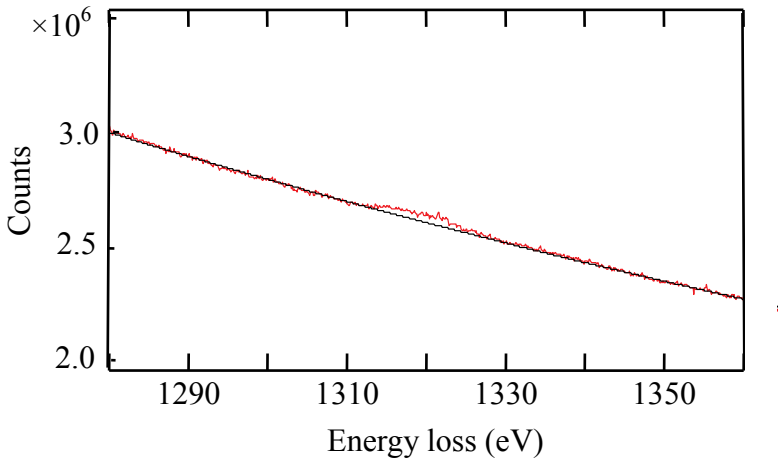

Fig. 10 Raw data (red line) of Mg K edge from a $LiNi_{0.8}Co_{0.15}Al_{0.05}(Mg_{0.05})lO_2$ thin foil sample, acquired with an exposure time of 30 s. The power law background is drawn to better observe the signal-to-background ratio.

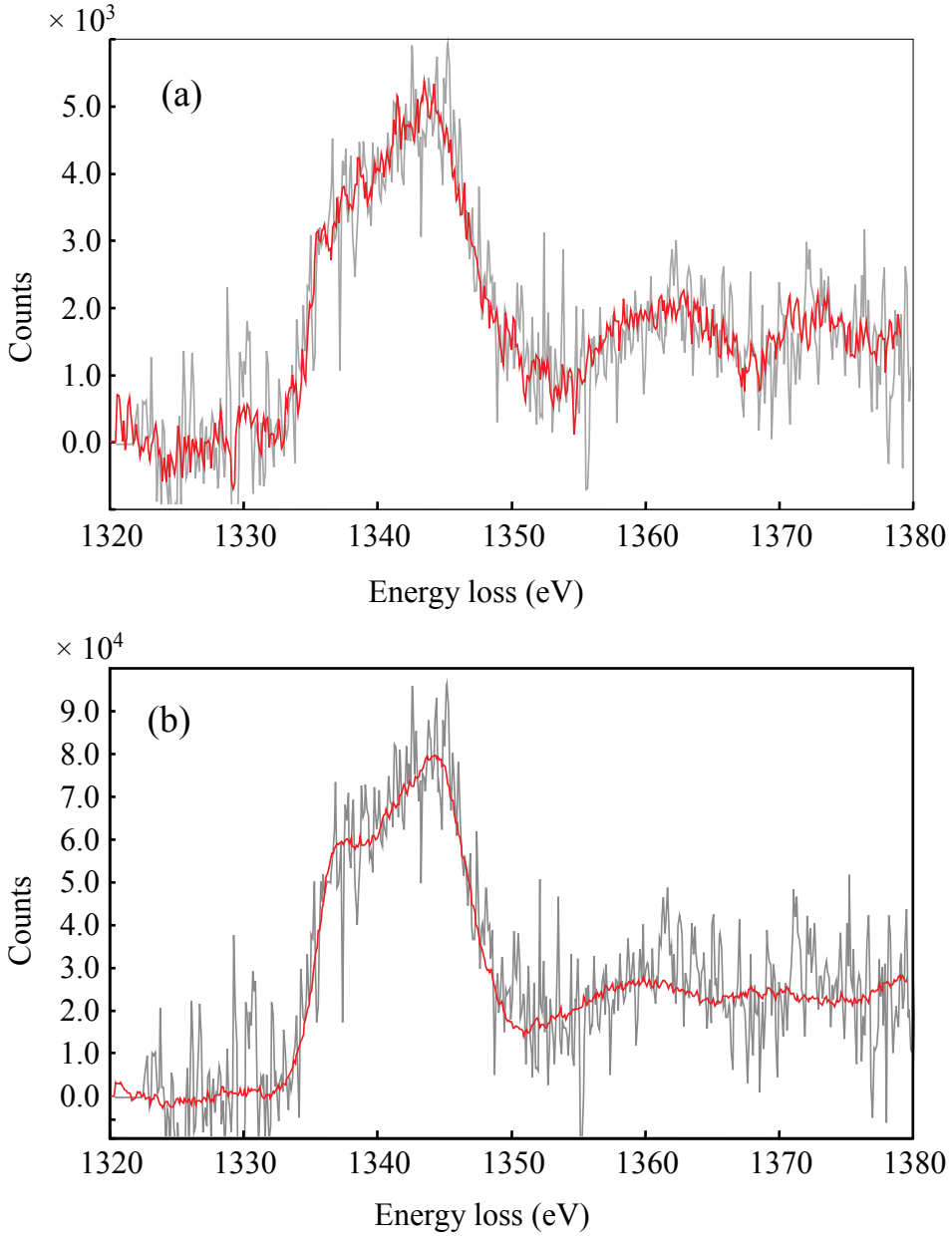

Fig. 11 Single acquisition with reduced intensity and an exposure time of 30 s (grey line, scaled by 10 times (a) and by 200 times (b)), final spectrum accumulated 10 (a) and 200 times (b), using the EDC_2 script (red line).

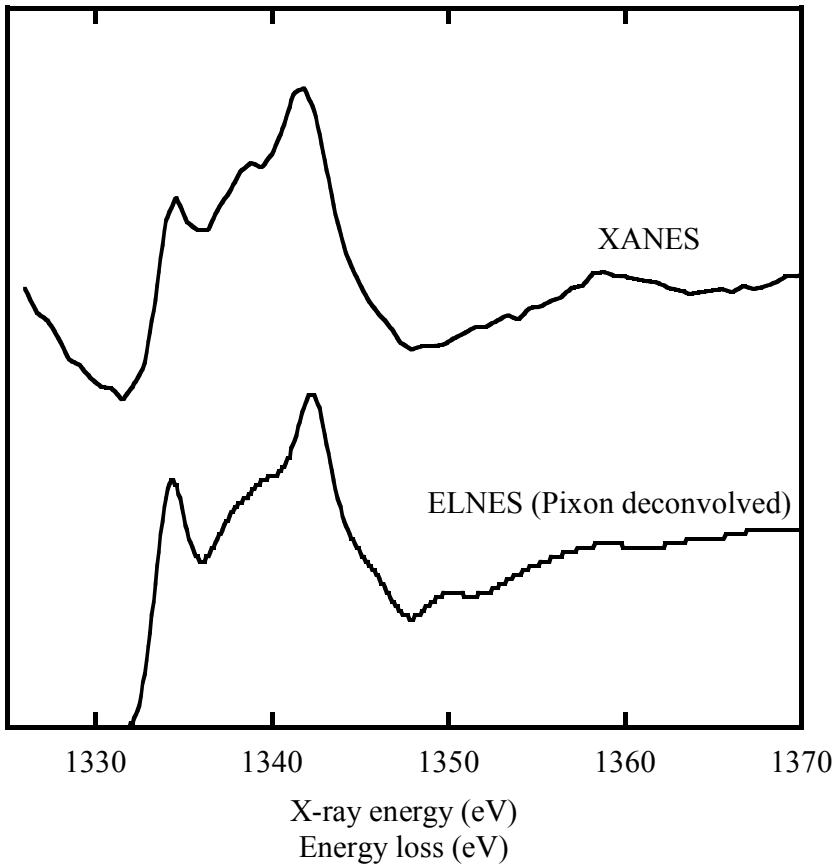

Fig. 12 Comparison between XANES spectrum taken from the $LiNi_{0.8}Co_{0.15}Al_{0.05}(Mg_{0.05})O_2$ powder [7] and ELNES of Fig. 11(b), deconvolved by the Pixon method to improve energy resolution.

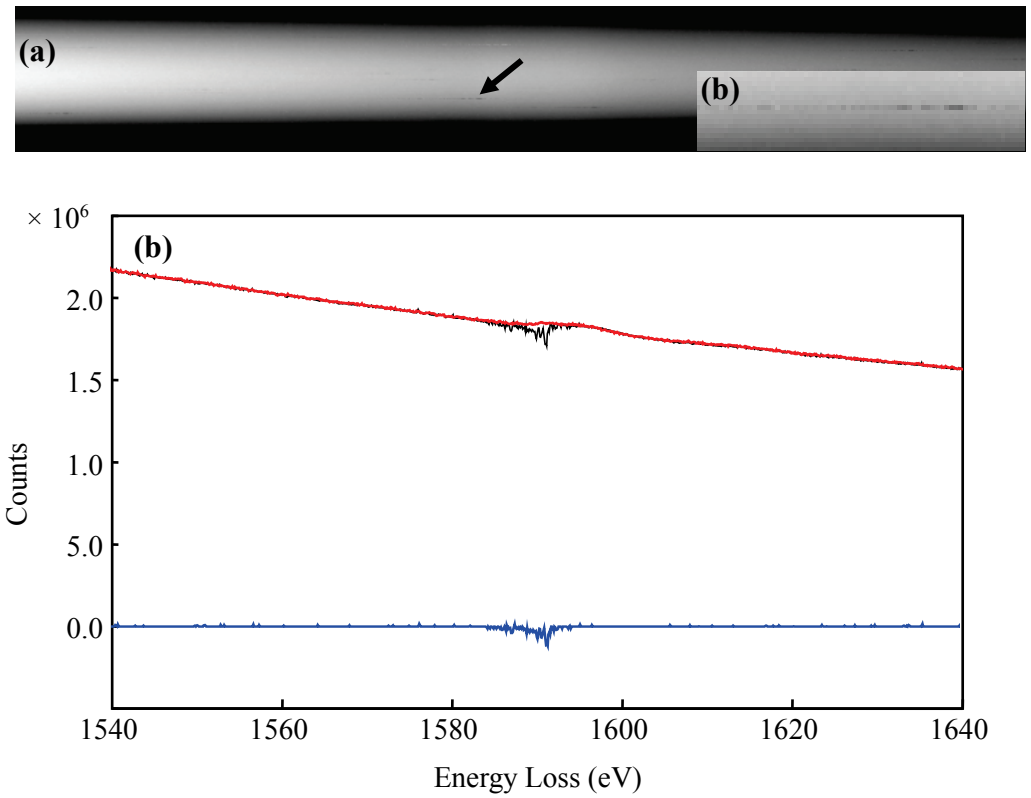

Fig. A-1(a) CCD image of EEL spectrum, accumulated using EDC_2 script. The arrow indicates the position of dark dots caused by spike noise while recording the gain reference image. (b) 1D projection of (a) in the cross dispersion direction (black line) and after spike removal (red line). The removed noise is also shown (blue line).